



Cite this: *Chem. Commun.*, 2019, 55, 12316

Received 12th August 2019,
Accepted 17th September 2019

DOI: 10.1039/c9cc03960k

rsc.li/chemcomm

Photoswitchable phthalocyanine-assembled nanoparticles for controlled “double-lock” photodynamic therapy†‡

Hong-Bo Cheng,^{§a} Xingshu Li,^{§a} Nahyun Kwon,^{§a} Yanyan Fang,^{*b} Gain Baek^a and Juyoung Yoon^{id *a}

In the current study, a new nanoparticle platform, NanoAzoPcS, is created by co-assembly of phthalocyanine and azobenzene amphiphiles, which can be used to gain precise control of PDT simply by regulating the stoichiometric ratio of the components and using light irradiation. The results of antibacterial studies show that NanoAzoPcS serves as a smart PS for controlled PDT.

Owing to its high spatiotemporal selectivity, photodynamic therapy (PDT) has become a clinically promising approach for the treatment of noninvasive cancers and microbial infections.¹ Upon light irradiation, preferably in the phototherapeutic window (650–850 nm), certain dyes (photosensitizers, PSs) are transformed to their triplet excited states through intersystem crossing (ISC) and then generate highly cytotoxic, short-lived reactive oxygen species (ROS).² The ROS and products of their chemical reactions only form at the time of irradiation and only in the region that is exposed to light. As a result, PDT possesses unique advantages associated with spatiotemporal selectivity, which benefit clinical applications.³ However, PDT suffers from several problems including the low water solubility of current molecular PSs (such as porphyrin and phthalocyanine), low photodynamic efficiency of nanostructured PSs and lack of efficient methods for delivery of PSs to target cells and tissues.⁴

Recently, supramolecular self-assemblies have emerged as promising tools in nanomedicine because they can serve as therapeutic nanosystems that can be controlled at the molecular level.⁵ Self-assembly of functional dyes is a versatile, “bottom-up” method for construction of nanodrugs for noninvasive cancer therapy and microbial infections.^{4b,6} Molecular aggregation plays

an important role in regulating the physical, chemical and/or biological properties of fluorescent dyes.⁷ Moreover, control of the packing of functional dyes in the supermolecular aggregates serves as a facile method to regulate and control photophysical properties. This feature enables the formation of new optical tools from individual dye molecules.⁸

Zinc(II) phthalocyanines (**ZnPcs**) have unique advantages for use in phototherapies, especially in medical applications of PDT, because they have long absorption wavelength maxima and high molar extinction coefficients.⁹ However, the fact that **ZnPcs** always exists in “on” states severely limits their use in PDT. In addition, control of the supramolecular assembly of **ZnPcs** is complex and uncertain. Precise regulation of the construction of assemblies of this type is critical to promote an efficient therapeutic effect and to have low side effects.

Moreover, because they have highly-conjugated organic structures, **ZnPcs** display poor water solubilities, which detracts from their use in clinical medicine.¹⁰ However, introducing hydrophilic groups into **ZnPcs** enhances their water solubilities. In earlier studies, we showed that amphiphilic analogues of phthalocyanines can be used in theranostic approaches owing to their high photodynamic activities toward cancer cells.¹¹

The concept of photopharmacology has been explored in the context of various therapeutic applications.¹² Azobenzenes, which have been used in photopharmacology,¹³ undergo well-known reversible N=N bond *E-Z* isomerization reactions that can be employed to control π - π stacking interactions.¹⁴ Because supramolecular coassembled nanoarchitectures have attracted increasing attention in the field of biomedicine, substances like azobenzenes that undergo π - π stacking have been screened to identify guests for forming coassembled nanoarchitectures with **ZnPcs**. However, to the best of our knowledge, activatable supramolecular coassembled azobenzenes/**ZnPcs**-based PDT systems that enable controlled ROS generation have not been developed to date.

In the study described below, we designed and synthesized several novel amphiphilic azobenzenes (**Azos**), and explored their ability to regulate the self-assembly behavior of 4-sulfonatophenoxy-substituted **ZnPcs** (Fig. 1). Moreover, we showed that the new

^a Department of Chemistry and Nano Science Ewha Womans University, Seoul 120-750, Korea. E-mail: jyoony@ewha.ac.kr

^b Beijing National Laboratory for Molecular Sciences, Key Laboratory of Photochemistry, Institute of Chemistry, Chinese Academy of Sciences, Beijing 100190, China. E-mail: fyy001@iccas.ac.cn

† This paper is dedicated to Prof. Eric V. Anslyn on the occasion of his 60th birthday.

‡ Electronic supplementary information (ESI) available. See DOI: 10.1039/c9cc03960k

§ These authors contributed equally to this work.

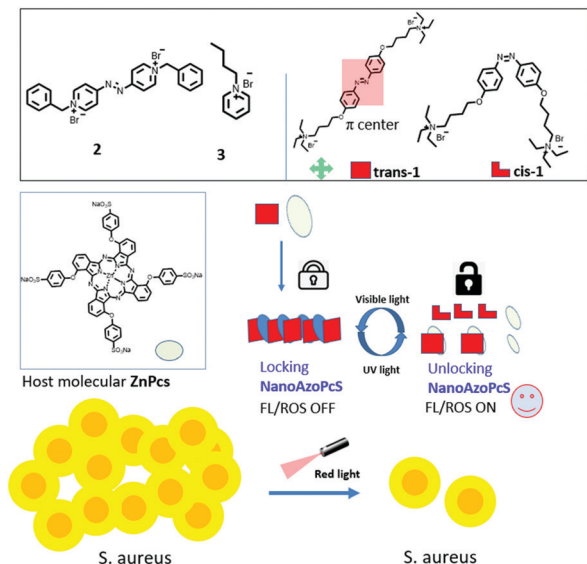


Fig. 1 Schematic illustration of the preparation of self-assembled **Azo-ZnPcs** nanoparticles (**NanoAzoPcs**) and their responsive disassembly to light for promotion of their photodynamic antibacterial effects.

nanoparticles, **NanoAzoPcs**, formed from **ZnPcs** and **Azos** can be used as light controlled antibactericidal agents.

The routes employed for the synthesis of **ZnPcs** and **Azos 1–3** are described in the ESI.† Several methods were used to examine the formation of host–guest nanosystems by mixing **ZnPcs** and **Azos 1–3**. Based on the results of calculations, which predict the strengths of π – π stacking interactions and molecular distances (Fig. 2a), **Azos 1** was expected to be an ideal guest for formation of coassembled host–guest nanosystems with **ZnPcs**. The binding affinities between **ZnPcs** and **Azos 1–3** were determined by using UV-vis titration. Inspection of Fig. 2b shows that addition of 2 equiv. of **Azo 1** to **ZnPcs** causes the greatest change in the absorption spectrum of **ZnPcs**. Interestingly, after addition of more than 2 equiv. of **Azo 1**, the intensity of the absorption of **ZnPcs** in the range of 600–800 nm undergoes decreases (Fig. 2c), which based on Kasha's exciton theory indicates that a decrease and broadening of the Q-band occurs. However, **Azos 2–3** induces only slight changes in the absorption spectrum of **ZnPcs** owing to unfavorable stacking and molecular distances, which decrease the propensity for complex formation (Fig. S5 and S6, ESI†).

Fluorescence changes caused by mixing host **ZnPcs** and guest **Azos 1–3** were explored in order to obtain information about aggregate generation. As shown in Fig. 2d and e, H-aggregates exist in the coassembled host–guest nanosystem **ZnPcs–Azo 1**. In addition, 2 equiv. of **Azo 1** induces the largest enhancement of **ZnPcs** fluorescence. Moreover, unlike **ZnPcs**, **NanoAzoPcs** (**ZnPcs/azo 1** = 5 μ M/35 μ M) does not fluoresce. This finding demonstrates that strong interactions occur between **ZnPcs** and **Azo 1** in the assembly. In striking contrast, **Azo 2** and **Azo 3** do not induce enhancements in the fluorescence of **ZnPcs** (Fig. S7 and S8, ESI†). Clearly, the combined results demonstrate that **Azo 1** interacts with **ZnPcs** most strongly to form a host–guest nanosystem.

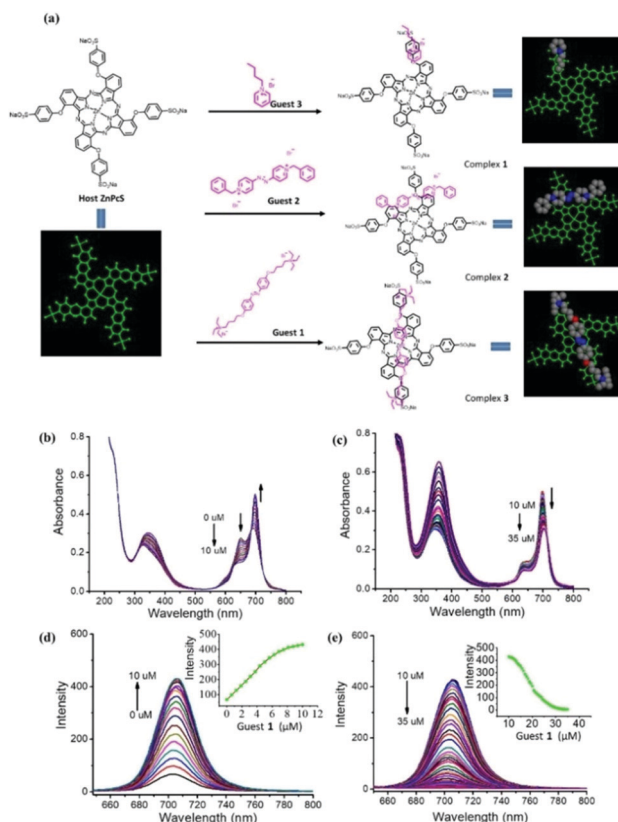


Fig. 2 (a) Models for assemblies of host **ZnPcs** and guest azobenzenes. Geometries were optimized by using the molecular mechanics and a dreiding force field. Simulations were performed using Material Studio software packages from Accelrys Inc. (b) Changes in the absorption spectrum of **ZnPcs** (5 μ M) in water in the presence of (b) 0–10 and (c) 10–35 μ M **Azo 1** (from). Changes in fluorescence spectrum of host **ZnPcs** (5 μ M) in water in the presence of (d) 0–10 and (e) 10–35 μ M of **Azo 1**.

Dynamic light scattering (DLS) analysis was used to monitor the formation of the coassembled host–guest nanosystems **ZnPcs–azo 1**. The results (Fig. 3a) show that pure **ZnPcs** and **NanoAzoPcs** (**ZnPcs/azo 1** = 5 μ M/5 μ M) in water have hydrodynamic diameters that are less than 20 nm. However, the assembly formed by mixing **ZnPcs** and 7 equiv. of **Azo 1** has a large mean hydrodynamic diameter of ca. 120 nm (Fig. 3b). Moreover, **NanoAzoPcs** (**ZnPcs/azo 1** = 5 μ M/35 μ M) in phosphate buffered solution (PBS) has a size distribution that is similar to that in water.

Transmission electron microscopy (TEM) was utilized to obtain more information about the formation of **NanoAzoPcs**. As can be seen by viewing the TEM images in Fig. 3c, **NanoAzoPcs** (**ZnPcs/azo 1** = 5 μ M/35 μ M) has an oval-shaped structure with a size of ca. 110 nm, which is in accordance with the size determined using DLS.

Stability and size distribution are key factors determining the practical utility of biomaterials. Hence, the stability of **NanoAzoPcs** (**ZnPcs/azo 1** = 5 μ M/35 μ M) in water and PBS was assessed. As can be seen by viewing the images in Fig. 3d, **NanoAzoPcs** is stable in both water and PBS. The high stability of **NanoAzoPcs** in PBS (physiological conditions) indicates its

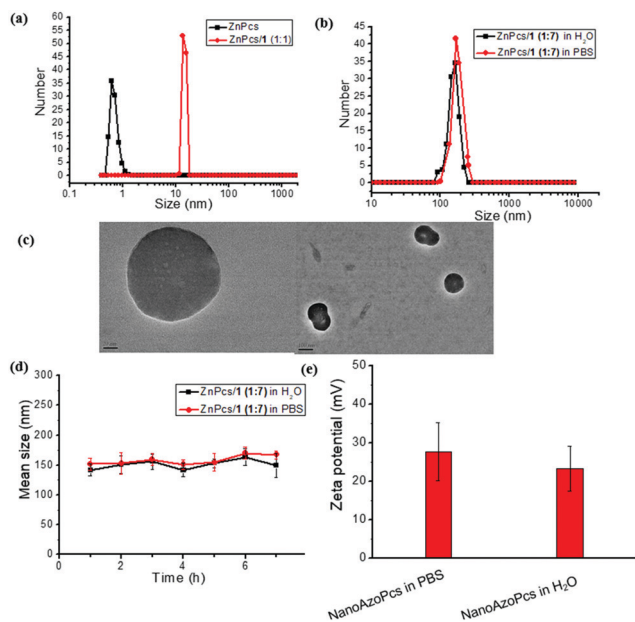


Fig. 3 Self-assembly to form **NanoAzoPcS** and its stability. (a) DLS size profiles for **ZnPcs** ($5 \mu\text{M}$) and **NanoAzoPcS** (**ZnPcs/azo 1** = $5 \mu\text{M}/5 \mu\text{M}$). (b) Size distribution of **NanoAzoPcS** (**ZnPcs/azo 1** = $5 \mu\text{M}/35 \mu\text{M}$) in water and PBS determined by using DLS. (c) The morphology of **NanoAzoPcS** (**ZnPcs/azo 1** = $5 \mu\text{M}/35 \mu\text{M}$) determined by using TEM. (d) Mean size of **NanoAzoPcS** (**ZnPcs/azo 1** = $5 \mu\text{M}/35 \mu\text{M}$) in water and in PBS after aging for different times detected by using DLS. (e) Zeta potential of **NanoAzoPcS** (**ZnPcs/azo 1** = $5 \mu\text{M}/35 \mu\text{M}$) in water and PBS.

potential for use in biomedical applications. The data in Fig. 3e show that the zeta potential of **NanoAzoPcS** is ca. +27 mV in water and ca. +23 mV in PBS, which indicates its high dispersion stability.

Azobenzene containing host-guest nanosystems have superior features for applications as supramolecular biomaterials. An important reason for this is that noncovalent interactions between azobenzenes and other substances can be controlled by using light.¹⁵ Therefore, disassembly of azobenzene based supramolecular assemblies has the capability of being triggered by an external light stimulus that promotes *E-Z* isomerization.¹⁶ The photophysical and photochemical properties of **NanoAzoPcS** were evaluated in order to determine if it can be employed as a light controlled PS for PDT. Analysis of the spectra shown in Fig. S9 and S10 (ESI[†]) indicates that an isosbestic point exists at 442 nm and that a significant decrease in the intensity of the absorption maximum at 358 nm occurs upon 365 nm irradiation. This observation shows that photoinduced *E-Z* isomerization occurs in the **azo 1** component. In addition, the absorption maximum of **NanoAzoPcS** at 355 nm undergoes a significant decrease while at the same time the intensity of the original absorption band in the 600–800 nm range is recovered.

Moreover, the intensity of fluorescence of **NanoAzoPcS** dramatically increases upon irradiation at 365 nm (Fig. 4d), which leads to disruption of π - π stacking between **ZnPcs** and **azo 1** (Fig. 4c). After three cycles of irradiation with UV (365 nm, for 1.0 min) and visible light (450 nm for 5.0 min), photo-switchable **NanoAzoPcS** maintains a high performance (Fig. 4d

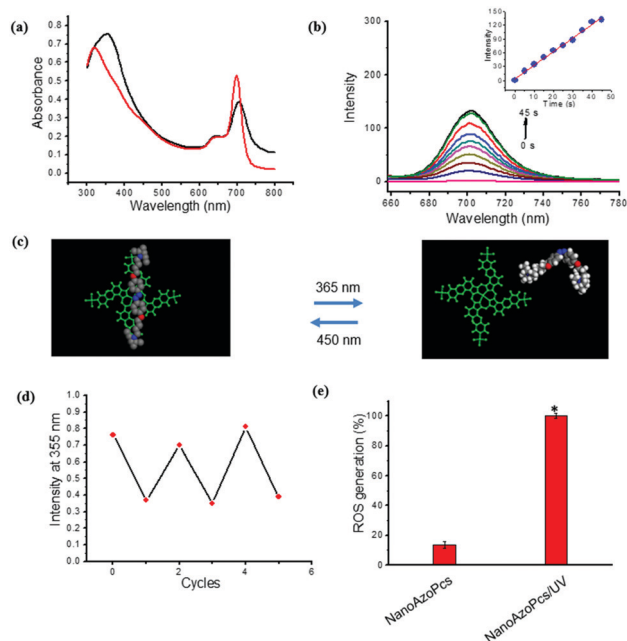


Fig. 4 Photoswitchable self-assembly process of **NanoAzoPcS** for controlled photoactivity. (a) Absorption and (b) fluorescence spectra (excited at 610 nm) of **NanoAzoPcS** (**ZnPcs/azo 1** = $5 \mu\text{M}/5 \mu\text{M}$) after photoirradiation at 365 nm. (c) Possible structures of the assembly of **NanoAzoPcS** after photoirradiation at 365 nm and then at 450 nm. (d) Changes in the fluorescence intensity of **NanoAzoPcS** (**ZnPcs/azo 1** = $5 \mu\text{M}/35 \mu\text{M}$) in water upon alternating UV (365 nm) and visible light (450 nm) irradiation. (e) ROS generation by (365 nm) UV irradiation of **NanoAzoPcS** (**ZnPcs/azo 1** = $5 \mu\text{M}/35 \mu\text{M}$) in water.

and Fig. S11, ESI[†]). It is known that singlet excited states of PSs undergo decay through three pathways including fluorescence emission, generation of heat through vibrational relaxation and production of the corresponding ROS forming triplet excited states by intersystem crossing (ISC). 2,7-Dichlorofluorescein diacetate was used as a probe in order to explore **NanoAzoPcS** (**ZnPcs/azo 1** = $5 \mu\text{M}/35 \mu\text{M}$) promoted generation of ROS in water. Importantly, the results show that 365 nm irradiation of **NanoAzoPcS** (**ZnPcs/azo 1** = $5 \mu\text{M}/35 \mu\text{M}$) leads to a significant increase in the formation of ROS such as $^1\text{O}_2$ (Fig. 4e and Fig. S12, S13, ESI[†]).

To assess the ability of **NanoAzoPcS** to serve as a novel nanoPS for PDT, we investigated its use in antibacterial photodynamic therapy (APDT). The Gram-negative bacteria *E. coli* and Gram-positive bacteria *S. aureus* in a nutrient medium were used as model biological targets. The results demonstrate that **NanoAzoPcS** (**ZnPcs/azo 1** = $5 \mu\text{M}/35 \mu\text{M}$) is well dispersed in water and PBS before and after irradiation with 365 nm light. A PBS solution of **NanoAzoPcS** was added to the *E. coli* and *S. aureus* cells and the cells were then incubated for 2 h. The Cryo TEM images of *S. aureus* bacterial cells show that small nanoparticles after dissociation of **NanoAzoPcS** (**ZnPcs/azo 1** = $5 \mu\text{M}/35 \mu\text{M}$) adhere to the surface of the bacterial cells (Fig. S14, ESI[†]). Following irradiation of the treated bacterial cells using a 655 nm laser (655 nm, 0.4 W cm^{-2} , 10 min), the cells were plated on LB agar plates and the plates were incubated

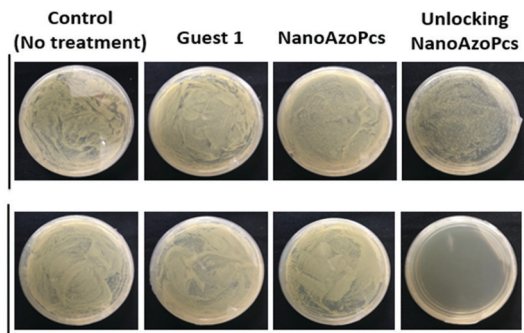


Fig. 5 Controlled photodynamic antibacterial effects. Photographs of plates containing *S. aureus* on LB agar treated with **Azo 1**, **NanoAzoPcs** (**ZnPcs/azo 1** = 5 $\mu\text{M}/35 \mu\text{M}$) and locking/unlocking **NanoAzoPcs** (**ZnPcs/azo 1** = 5 $\mu\text{M}/35 \mu\text{M}$) under laser irradiation. Control groups are untreated bacteria. Laser conditions: 655 nm, 0.4 W cm^{-2} , 10 min.

for 12 h in the dark. Inspection of the images in Fig. 5 shows that the **Azo 1** and **NanoAzoPcs** do not promote inhibition of bacterial growth both in the absence and presence of 655 nm laser irradiation. However, unlocking **NanoAzoPcs** (**ZnPcs/azo 1** = 5 $\mu\text{M}/35 \mu\text{M}$) does have inhibitory effects on the growth of 655 nm laser irradiated *E. coli* and *S. aureus* cells (Fig. 5 and Fig. S15, ESI \ddagger). Moreover, as can be seen by viewing Fig. S16 (ESI \ddagger), the antibacterial activity of unlocked **NanoAzoPcs** (**ZnPcs/azo 1** = 5 $\mu\text{M}/35 \mu\text{M}$) is concentration dependent in the tested range of 100–1000 nM. The number of colony forming units (CFUs) was used to determine the numbers of live *S. aureus* bacterial cells. Inspection of Fig. S16 (ESI \ddagger) shows that “double-lock” **NanoAzoPcs** has antibacterial effects on *S. aureus* in the range of 100–1000 nM.

In summary, in this effort we synthesized a nanostructured PS by co-assembling a phthalocyanine derivative and an azobenzene amphiphile. We showed that the activity of the nanostructured PS can be controlled by varying the stoichiometric ratios of the components and using isomerization of azobenzene. The novel self-assembled phthalocyanine-azobenzene containing nanoPS effectively promotes the death of red light irradiated bacteria cells. Thus, combining the photosensitizer **ZnPcs** with the photochromic switchable **azo 1** component leads to the formation of a PS system that exists in an “off” state and that can be transformed to active state for “double-lock” PDT. The host–guest nanosystem developed in this effort should serve as a model to guide the design of general photoactivatable based strategies to overcome current limitations of PDT.

J. Y. is thankful for financial support from the National Research Foundation of Korea (NRF), which is funded by the Korea government (MSIP) (No. 2012R1A3A2048814).

Conflicts of interest

There are no conflicts to declare.

Notes and references

- (a) H.-B. Cheng, Y. Cui, R. Wang, N. Kwon and J. Yoon, *Coord. Chem. Rev.*, 2019, **392**, 237–254; (b) S. S. Lucky, K. C. Soo and Y. Zhang, *Chem. Rev.*, 2015, **115**, 1990–2042; (c) S. Monro, K. L. Colon, H. Yin, J. Roque, P. Konda, S. Gujar, R. P. Thummel, L. Lilge, C. G. Cameron and S. A. McFarland, *Chem. Rev.*, 2019, **119**, 797–828; (d) A. P. Castano, P. Mroz and M. R. Hamblin, *Nat. Rev. Cancer*, 2006, **6**, 535–545; (e) K. K. Ng and G. Zheng, *Chem. Rev.*, 2015, **115**, 11012–11042.
- (a) L. Cheng, C. Wang, L. Feng, K. Yang and Z. Liu, *Chem. Rev.*, 2014, **114**, 10869–10939; (b) X. Li, D. Lee, J.-D. Huang and J. Yoon, *Angew. Chem.*, 2018, **130**, 10033–10038; (c) X. S. Li, S. Kolemen, J. Yoon and E. U. Akkaya, *Adv. Funct. Mater.*, 2017, **27**, 1604053; (d) H. Yuan, B. Wang, F. Lv, L. Liu and S. Wang, *Adv. Mater.*, 2014, **26**, 6978–6982.
- (a) W. Fan, P. Huang and X. Chen, *Chem. Soc. Rev.*, 2016, **45**, 6488–6519; (b) V. Shanmugam, S. Selvakumar and C. S. Yeh, *Chem. Soc. Rev.*, 2014, **43**, 6254–6287.
- (a) V. Almeida-Marrero, E. van de Winckel, E. Anaya-Plaza, T. Torres and A. de la Escosura, *Chem. Soc. Rev.*, 2018, **47**, 7369; (b) X. Li, B.-D. Zheng, X.-H. Peng, S.-Z. Li, J.-W. Ying, Y. Zhao, J.-D. Huang and J. Yoon, *Coord. Chem. Rev.*, 2019, **379**, 147.
- (a) H.-B. Cheng, Y.-M. Zhang, Y. Liu and J. Yoon, *Chem*, 2019, **5**, 553; (b) J. Wang, K. Liu, R. Xing and X. Yan, *Chem. Soc. Rev.*, 2016, **45**, 5589; (c) L. Yang, X. Tan, Z. Wang and X. Zhang, *Chem. Rev.*, 2015, **115**, 7196; (d) G. Yu, B. C. Yung, Z. Zhou, Z. Mao and X. Chen, *ACS Nano*, 2018, **12**, 7; (e) J. Zhou, G. Yu and F. Huang, *Chem. Soc. Rev.*, 2017, **46**, 7021.
- (a) H. Cheng, J. Yoon and H. Tian, *Coord. Chem. Rev.*, 2018, **372**, 66; (b) H.-B. Cheng, H.-Y. Zhang and Y. Liu, *J. Am. Chem. Soc.*, 2013, **135**, 10190; (c) Y. Liu, P. Bhattarai, Z. Dai and X. Chen, *Chem. Soc. Rev.*, 2019, **48**, 2053.
- (a) H. B. Cheng, Z. Sun, N. Kwon, R. Wang, Y. Cui, C. O. Park and J. Yoon, *Chem. – Eur. J.*, 2019, 3501; (b) A. S. Weingarten, R. V. Kazantsev, L. C. Palmer, M. McClendon, A. R. Koltonow, A. P. S. Samuel, D. J. Kiebal, M. R. Wasielewski and S. I. Stupp, *Nat. Chem.*, 2014, **6**, 964; (c) S. Yagai, S. Okamura, Y. Nakano, M. Yamauchi, K. Kishikawa, T. Karatsu, A. Kitamura, A. Ueno, D. Kuzuhara, H. Yamada, T. Seki and H. Ito, *Nat. Commun.*, 2014, **5**, 4013.
- S. Cheung and D. F. O’Shea, *Nat. Commun.*, 2017, **8**, 1885.
- R. C. H. Wong, P. C. Lo and D. K. P. Ng, *Coord. Chem. Rev.*, 2019, **379**, 30.
- (a) D. K. Ng and J. Jiang, *Chem. Soc. Rev.*, 1997, **26**, 433; (b) R. C. H. Wong, S. Y. S. Chow, S. Zhao, W. P. Fong, D. K. P. Ng and P. C. Lo, *ACS Appl. Mater. Interfaces*, 2017, **9**, 23487.
- X. Li, S. Yu, Y. Lee, T. Guo, N. Kwon, D. Lee, S. C. Yeom, Y. Cho, G. Kim, J. D. Huang, S. Choi, K. T. Nam and J. Yoon, *J. Am. Chem. Soc.*, 2019, **141**, 1366.
- F. Xiao, B. Cao, C. Wang, X. Guo, M. Li, D. Xing and X. Hu, *ACS Nano*, 2019, **13**, 1511.
- (a) M. M. Lerch, M. J. Hansen, G. M. van Dam, W. Szymanski and B. L. Feringa, *Angew. Chem., Int. Ed.*, 2016, **55**, 10978; (b) M. Wegener, M. J. Hansen, A. J. M. Driessen, W. Szymanski and B. L. Feringa, *J. Am. Chem. Soc.*, 2017, **139**, 17979.
- E. C. Carroll, S. Berlin, J. Levitz, M. A. Kienzler, Z. Yuan, D. Madsen, D. S. Larsen and E. Y. Isacoff, *Proc. Natl. Acad. Sci. U. S. A.*, 2015, **112**, E776.
- H.-B. Cheng, Y.-M. Zhang, C. Xu and Y. Liu, *Sci. Rep.*, 2014, **4**, 4210.
- A. A. Beharry and G. A. Woolley, *Chem. Soc. Rev.*, 2011, **40**, 4422.